Electromagnetic Scattering by Metallic Holes and Its Applications in Microwave Circuit Design

Ali Zeid, *Associate Member, IEEE,* and Henri Baudrand, *Senior Member, IEEE*

***Abstract*—The problem of arbitrarily incident plane-wave scattering from rods structures of thick conducting plates arranged with two-dimensional (2-D) periodicity has been examined. The square approximation as well as truncated-square approximation of circular cross sections is used in this study. The impedance of cascaded screens and the reflection coefficient is calculated using the multimodal variational method for both TE- and TM-polarized incident electric field. The 2-D periodic structure of holes described in this paper can be used for the purpose of designing new guiding microwave structures. A transverse resonance method is applied to solve this problem. The convergence behavior of the technique has also been examined. The numerical results of the reflection coefficient, surface impedance, and dispersion curves are presented.**

I. Introduction

PERIODIC screens are used in many applications for science and engineering over a wide range of the electromagnetic spectrum. An infinite array of metallic rods or strips, such as illustrated in Fig. 1, forms a useful model for the analysis of many practical microwave structures such as filters, lenses, and artificial dielectrics [1]. A knowledge of the reflection and transmission coefficients at the array surface is required in each of these applications.

The problem of scattering by a two-dimensional (2-D) periodic array of rectangular plates was investigated by Ott *et al.* [2]. They used the point matching method to solve the integral equation for the unknown current on the plate. The solution given is restricted to the case of narrow plates arranged in a rectangular lattice with a normal incident plane wave. The complementary problem of scattering by a conducting screen periodically perforated with apertures was treated by Kieburtz and Ishimaru [3] by the variational method. The accuracy of the variational solution depends on the ability to choose an appropriate trial function. Accomplishment by the cascade connection of components as characterized by their scattering parameters, surfaces, and dielectric layers are treated as distinct elements with the cascade connection of their scattering parameters found from standard microwave analysis extended to field quantities [4]. Rubin examined the effect of thickness on periodic structures by analyzing the scattering from a one-dimensional (1-D) array of thick bars [5] and a 2-D array of thick patches [6] since the thickness of the structure stemmed from that of the patch itself.

In this paper, the problems of electromagnetic isolation between elements of microelectronic circuits have been studied.

Manuscript received July 22, 1999; revised November 23, 2000.

A. Zeid is with the Electronic Laboratory, Department of Telecommunication, University of Allepo, Allepo, Syria.

H. Baudrand is with ENSEEHIT, F-31071 Toulouse, France.

Publisher Item Identifier S 0018-9480(02)03021-1.

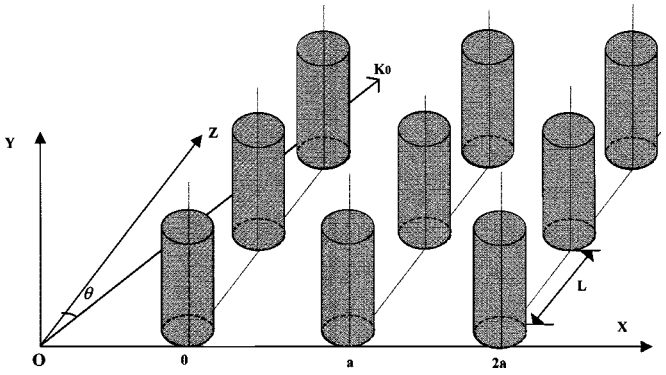

Fig. 1. Geometry of metallic plates (cascaded arrangement) ($a = 1$ mm, $L = 0.05$ mm, θ).

Metallic rods disposed periodically in cascade have been treated. A metallic slab of square or truncated square cross-section approximates each metallic slab of a circular cross section. By using the truncated square approximation, the difference between the origin cross section and this approximation is optimized. The surface impedance Z_{11} and the reflection coefficient S_{11} are computed by the multimodal variational method. A comparison between the two approaches, in the case of a TE field, has been illustrated for square and truncated square cross sections. The study of the dispersion curves between two grids of periodically arranged metallic holes allows the fabrication of the waveguide. In Sections II–VI, theoretical background, calculation of the impedance matrix, determination of the trial functions, the equivalent-circuit representation, and the application of the multimodal variational method are demonstrated. A waveguide design between two grids of periodically arranged metallic holes is then illustrated. Finally, the numerical results and conclusions are explained.

II. Theoretical Background

The problem under consideration consists of an incident plane wave on metallic plates, as shown in Fig. 2. The metallic slabs have infinite lengths and space regularity. The axis of plates are parallel to oy and periodic in the ox-direction. The period in the x-direction is a. The incident plane wave has a propagation vector making an angle of θ with respect to the z-axis. The electromagnetic fields must satisfy the requirements imposed by Floquet's theorem. The plane wave in the transverse directions may be TM or TE. The time dependence $e^{j\omega t}$ is omitted. The scalar mode functions can be defined as in [7] and [8] as follows:

$$\phi_n = ce^{-j\beta_x x}e^{-j\beta_y y}e^{-jk_z z}. \tag{1}$$

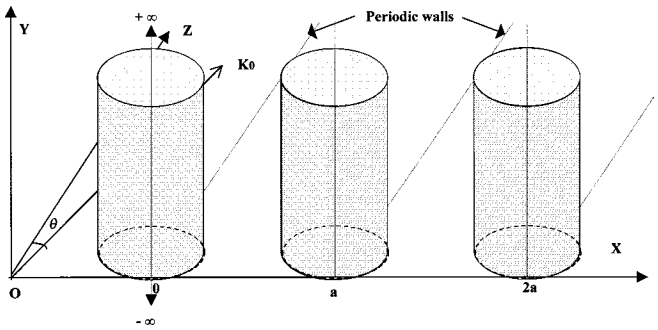

Fig. 2. Geometry of the problem (periodic: $a = 1$ mm).

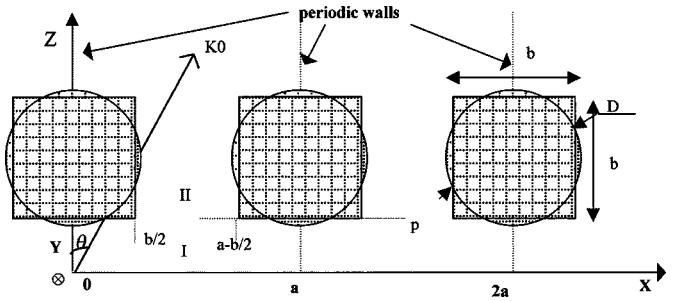

Fig. 3. Discontinuity plane of square metallic plate ($a = 1$ mm, $b = 0.1$ mm, θ).

The propagation of the wave is independent of the y-direction so (1) can be rewritten as

$$\phi_n = ce^{-j\beta_x x}e^{-jk_z z} \tag{2}$$

where the associated transverse propagation constant is

$$\beta_x = k_0 \sin\theta + \frac{2n\pi}{a} \tag{3}$$

and $k_0 = \omega\sqrt{\varepsilon_0\mu_0}$ is the free-space wavenumber and c is a constant, which can be evaluated by using the normalization condition.

The scalar mode functions ϕ_n must satisfy the Helmholtz equation. With proper boundary conditions, the propagation constant in the z-direction can be defined as

$$k_z = \begin{cases} \sqrt{k_0^2 - (\beta_x)^2}, & \text{when } k_0^2 > \beta_x^2 \\ -j\sqrt{(\beta_x)^2 - k_0^2}, & \text{when } k_0^2 < \beta_x^2. \end{cases} \tag{4}$$

Therefore, the TE field for the TE mode is written as follows:

$$E_y = -\frac{1}{\sqrt{a}}e^{-j(k_0 \sin\theta + 2n\pi/a)x}e^{-jk_z z}. \tag{5}$$

The TE field of the TM mode can be also written as

$$E_x = \frac{1}{\sqrt{a}}e^{-j(k_0 \sin\theta + 2n\pi/a)x}e^{-jk_z z}. \tag{6}$$

III. Impedance Matrix of Metallic Holes

To calculate the impedance matrix, either an electric or magnetic wall must be imposed at the center of the slab. When the discontinuity problem has geometrical symmetry, the solution can be split into even and odd parts by introducing magnetic and electric walls, respectively, at the symmetry plane, as described for the thick iris resolution by Collin [1] and Rozzi [9], [10], respectively.

The relationship between tangential electric fields and current densities infinitely close to two surfaces is [11]

$$\begin{bmatrix} E_1 \\ E_2 \end{bmatrix} = \begin{bmatrix} Z_{11} & Z_{12} \\ Z_{12} & Z_{11} \end{bmatrix} \cdot \begin{bmatrix} J_1 \\ J_2 \end{bmatrix} \tag{7}$$

where E is the electric field and J is the current related to the magnetic field by $J_i = H_i \times n_i$ [12].

When the magnetic and electric walls are introduced, the even and odd solutions for the reduced driving point impedances Z_{even} and Z_{odd} can be obtained in a manner similar to [1]; the resultant two-port network (7) is then characterized by

$$Z_{11} = \frac{Z_{\text{even}} + Z_{\text{odd}}}{2} \text{ and } Z_{12} = \frac{Z_{\text{even}} - Z_{\text{odd}}}{2}. \tag{8}$$

Finally, the scattering matrix of the metallic holes can be obtained by the following expression:

$$S = (z+u)^{-1}(z-u) \tag{9}$$

where $[z]$ is the reduced impedance matrix and $[u]$ is the identity matrix.

IV. Microwave Scattering by Square Plates

The choice of a complete trial function is based on the electromagnetic field into region II [12], as shown in Fig. 3. The structure of this region is determined by electric walls at $x = b/2$ and at $x = a - b/2$.

By using the boundary conditions of the structure, the trial function in case of the TE mode can be written as

$$E_y = -\sqrt{\frac{t_n}{a-b}}\sin\frac{p\pi x}{a-b}e^{-jk_z z} \tag{10}$$

and also for the TM modes as

$$E_x = \sqrt{\frac{t_n}{a-b}}\cos\frac{p\pi x}{a-b}e^{-jk_z z} \tag{11}$$

where

$$t_n = \begin{cases} t_n = 1, & \text{if } p = 0 \\ t_n = 2, & \text{if } p \neq 0 \end{cases}$$

and where a is the period in x and b is the dimension of square plate.

The generalized trial quantity in the equivalent network representation of the boundary conditions are required on the overall domain as virtual adjustable sources [11]–[14]. The domain of the trial quantity, the boundary conditions on a plane of discontinuity, the equivalent network representation of the discontinuity domain, and the definition of the trial quantity are established in [12], [13], and [15]. Here, the trial function chosen is the electric field E. The representation of modal current source in the current density J_0 of the fundamental mode in the waveguide is presented in [12], [13], and [15]. Let us consider $\hat{Y}_1$, the admittance operator that describes the contribution of the evanescent

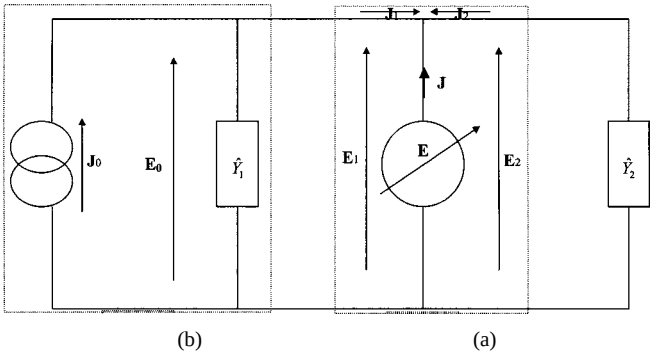

Fig. 4. Equivalent circuit of the configuration of discontinuity of square plate. (a) Representation of the discontinuity domain. (b) Representation of modal current source in a network.

mode on the current density, and $\hat{Y}_2$, the admittance operator of a short or open circuit according to the symmetric or antisymmetric plane [13], [16], [19]. Therefore, the equivalent circuit of the discontinuity for square plates in Fig. 3 is shown in Fig. 4. The solution has been derived by applying analogies of Kirchoff's and Ohm's laws to the equivalent network representation of Fig. 4. A matrix form can be deduced as follows:

$$\begin{bmatrix} E_0 \\ J \end{bmatrix} = \begin{bmatrix} 0 & 1 \\ -1 & \hat{Y}_1 + \hat{Y}_2 \end{bmatrix} \begin{bmatrix} J_0 \\ E \end{bmatrix} \tag{12}$$

where the right-hand side contains the real and virtual sources and the left-hand side contains the dual quantities. By applying Galerkin's method to (12), the following matrix equation can be written:

$$\begin{bmatrix} V_0 \\ 0 \end{bmatrix} = \begin{bmatrix} 0 & \overbrace{\langle f_0, g_1\rangle \quad \cdots \quad \langle f_0, g_p\rangle}^{A^t} \\ \overbrace{-\langle g_1, f_0\rangle}^{A} & \\ \vdots & \left\langle g_q, \left(\hat{Y}_{1n} + \hat{Y}_{2p}\right) g_p \right\rangle \\ -\langle g_q, f_0\rangle & \end{bmatrix} \begin{bmatrix} I_0 \\ [X] \end{bmatrix} \tag{13}$$

where $V_0 = E_0 f_0$, $I_0 = J_0 f_0$, and E is replaced by

$$E = \sum_p X_p \cdot g_p, \quad \langle g_p, J\rangle = 0, \qquad \text{for all } p. \tag{14}$$

The last three equations can be found in [11], [14]–[16]. From the matrix (13), an impedance Z can be deduced as

$$Z = A^t [Y]^{-1} A \tag{15}$$

where $[Y]$ is the admittance operator of square metallic plates, which is given by

$$[Y]_{qp} = \sum_{n\geq 1}^{N} \langle g_q, f_n\rangle \cdot Y_{1n} \langle f_n, g_p\rangle + Y_2 \cdot \delta_{qp} \tag{16}$$

where

$$\delta_{qp} = \begin{cases} 0, & \text{if } p \neq q \\ 1, & \text{if } p = q. \end{cases}$$

In the plane of the discontinuity, an infinite number of modes are excited, but in the case of several cascaded discontinuities, only a few of them are "seen" by the neighboring discontinuities. These are the so-called "accessible" modes and have the lowest cutoff frequency. The other modes are "localized" in the discontinuity. All ports corresponding to localized modes have been terminated by their modal characteristic admittance [9]. By utilizing the multimodal variational formulation [18], [19], the formulation of the particular problem (15) and (16) can be written as

$$Z_k = A_k^t [Y]^{-1} A_k \tag{17}$$

where k is considered as a number of accessible modes and $[Y]$ is the admittance operator of square metallic plates given by

$$[Y]_{qp} = \sum_{n=k+1}^{N} \langle g_p, f_n\rangle Y_{1n} \langle f_n, g_p\rangle + Y_2 \delta_{qp} \tag{18}$$

and

$$A_k^t = \begin{bmatrix} \langle f_0, g_1\rangle & \cdots & \langle f_0, g_p\rangle \\ \langle f_k, g_1\rangle & \cdots & \langle f_k, g_p\rangle \end{bmatrix}.$$

Finally, the expression of the impedance matrix (8) of the thick plates can be expressed as $[Z_k]$. The scattering matrix of the plates is then obtained by the following expression:

$$S_k = (z_k + u)^{-1}(z_k - u) \tag{19}$$

where z_k is the reduced impedance and u is the unit matrix.

Compared to the generalized scattering matrix method (GSMM), the advantage of our approach resides in using the notions of structures involving several cascaded discontinuities is obtained by chaining the S-matrix of every discontinuity according to the well-known formulas [20]. While the GSMM uses matrices whose dimensions depend on the number of considered mode in every discontinuity, the variational approach involves matrices with much smaller dimensions because it considers only the number of accessible modes. Since the localized modes are taken into account in a summation, it is possible to use a large number of them with a reasonable computation time [19].

V. Microwave Scattering by Truncated Square Plates

The second case of study is the truncated square form. This arrangement is close to the circular form. There is very little difference between the two forms. Due to this approximation, there are two discontinuities. To find the trial function of the first discontinuity (p_1), it must be put on electric wall at $x = b/2$ and $x = a - b/2$. For the second discontinuity (p_2), the trial function can be determined with electric walls at $x = b/2 + d$ and $x = a - (b/2 + d)$, as shown in Fig. 5.

By applying the boundary conditions as in the previous case, the trial functions for the TE and TM modes of the first discontinuity will have the same forms as in (10) and (11), respectively. For the second discontinuity, the trial functions can be expressed as

$$E_y = -\sqrt{\frac{t_n}{a-c}} \sin \frac{p\pi x}{a-c} e^{-jk_z z} \tag{20}$$

$$E_x = \sqrt{\frac{t_n}{a-c}} \cos \frac{p\pi x}{a-c} e^{-jk_z z} \tag{21}$$

where $c = b + 2d$.

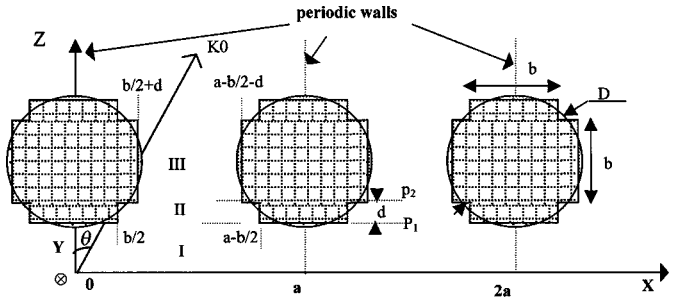

Fig. 5. Discontinuity plane of truncated square metallic plate ($a = 1$ mm, $b = 0.072$ mm, $d = 0.017$ mm, θ).

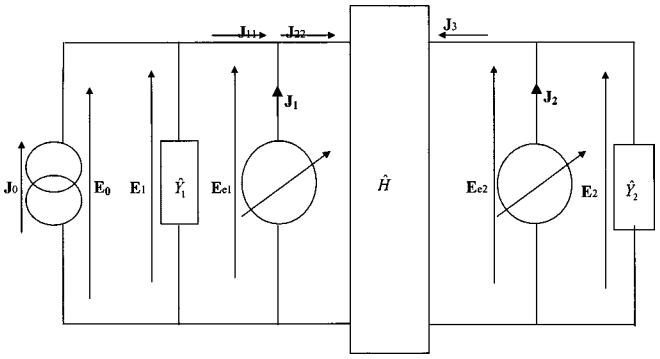

Fig. 6. Equivalent circuit of the configuration of discontinuity of truncated square plate.

The equivalent circuit of the second structure in Fig. 5 is shown in Fig. 6. In the same manner, the solution has been derived from the analogy of Kirchoff's and Ohm's laws applied to the equivalent network representation of Fig. 6. The equations can be written in a matrix form as follows:

$$\begin{bmatrix} E_0 \\ J_1 \\ J_2 \end{bmatrix} = \begin{bmatrix} 0 & 1 & 0 \\ -1 & \hat{Y}_1 + \hat{H}_{11} & \hat{H}_{12} \\ 0 & \hat{H}_{21} & \hat{H}_{22} + \hat{Y}_2 \end{bmatrix} \begin{bmatrix} J_0 \\ E_{e1} \\ E_{e2} \end{bmatrix} \tag{22}$$

where $\hat{H}$ is an admittance operator of a length of line that permits the passage from the first discontinuity p_1 to the second p_2.

As in the previous case, by considering k the number of accessible modes and by applying Galerkin's method, the impedance matrix can be written as

$$Z_k = B_k^t [Y]^{-1} B_k \tag{23}$$

where $[Y]$ is the admittance operator for the truncated square metallic plates, which is written as the following expression:

$$[Y]_{q1p1} = \sum_{n=k+1}^{N} \left\langle g_{q1}, \left(\hat{Y}_1 + \hat{H}_{11}\right) g_{p1} \right\rangle - \left\langle g_{q1}, \hat{H}_{12} g_{p2} \right\rangle \times \left(\left\langle g_{q2}, \left(\hat{H}_{22} + \hat{Y}_2\right) g_{p2} \right\rangle \right)^{-1} \left\langle g_{q2}, \hat{H}_{21} g_{p1} \right\rangle \tag{24}$$

and

$$B_k^t = \begin{bmatrix} \langle f_{01}, g_{11} \rangle & \cdots & \langle f_{01}, g_{p1} \rangle \\ \langle f_{k1}, g_{11} \rangle & \cdots & \langle f_{k1}, g_{p1} \rangle \end{bmatrix}.$$

VI. Cascaded Discontinuities Analysis

In general, the cascaded metal plates and dielectric slabs are used to obtain the desired transmission characteristics.

The calculation of the cascaded discontinuities in Fig. 1 was done by [21]. A matrix of a length of line l for an nth-order mode, which permits the passage from the first to the second slab, is used. The impedance matrix of a length of line l for the k number of accessible modes is given by

$$[Z] = \begin{bmatrix} [Z_m \cdot \coth \gamma_n l] & \left[\dfrac{Z_m}{\sinh \gamma_n l}\right] \\ \left[\dfrac{Z_m}{\sinh \gamma_n l}\right] & [Z_m . \coth \gamma_n l] \end{bmatrix} \tag{25}$$

where Z_m is the impedance of the accessible modes k.

In order to assemble various discontinuities that are obtained by a chain $[z]$ matrix, two multiple of impedance matrices $[Z_a]$ and $[Z_b]$ are considered as follows:

$$[Z_a] = \begin{bmatrix} [Z_{a11}] & [Z_{a12}] \\ [Z_{a21}] & [Z_{a22}] \end{bmatrix} \quad [Z_b] = \begin{bmatrix} [Z_{b11}] & [Z_{b12}] \\ [Z_{b21}] & [Z_{b22}] \end{bmatrix} \tag{26}$$

where all the sub-matrices that compose the matrices $[Z_a]$ and $[Z_b]$ can be expressed in terms of the accessible modes k. The $[z]$ matrix is expressed as

$$[Z] = \begin{bmatrix} [Z_{11}] & [Z_{12}] \\ [Z_{21}] & [Z_{22}] \end{bmatrix} \tag{27}$$

where

$$[Z_{11}] = [Z_{a11}] - [Z_{a12}] \cdot [Y_{ab}] \cdot [Z_{a21}] \tag{28}$$

$$[Z_{12}] = [Z_{a12}] \cdot [Y_{ab}] \cdot [Z_{b21}] \tag{29}$$

$$[Z_{21}] = [Z_{b21}] \cdot [Y_{ab}] \cdot [Z_{a21}] \tag{30}$$

$$[Z_{22}] = [Z_{b11}] - [Z_{b12}] \cdot [Y_{ab}] \cdot [Z_{b21}] \tag{31}$$

$$[Y_{ab}] = \Big([Z_{a22}] + [Z_{b11}] \Big)^{-1}. \tag{32}$$

VII. Waveguide Design Between Two Grids of Periodically Arranged Metallic Holes

An electromagnetic wave of perpendicular polarization arrives on an electric conducting level at $x = 0$ with an angle of incidence θ_{in}. Medium 1 is air. The factor of reflection is worth -1 then, and the total electric field in the air is given by [22]

$$\underline{E}(x,z) = -2j\, e_z \underline{E}_{zi}(0) \sin(\beta_1 x \sin\theta_{\text{in}}) \cdot e^{(-j\beta_1 z \cos\theta_{\text{in}})}. \tag{33}$$

Also, the magnetic field in medium 1 (air) is defined as

$$\underline{H}(x,z) = 2\underline{E}_{zi} \frac{\beta_1}{\omega \cdot \mu_0} [-j e_z \cos\theta_{\text{in}} \sin(\beta_1 x \sin\theta_{\text{in}}) + e_x \sin\theta_{\text{in}} \cos(\beta_1 x \sin\theta_{\text{in}})] e^{(-j\beta_1 z \cos\theta_{\text{in}})}. \tag{34}$$

It is noted that the boundary condition at the edge of the perfect electric conductor in the $x = 0$ plane is indeed satisfied (the tangential electric field is equal to zero, and the normal component of the induction field $\mu_0 \cdot H$ is zero). In addition, it is noted that the fields have a periodic dependence in x, and these conditions are also satisfied on all the parallel planes located at a distance x_m from the first plane

$$x_m = \frac{m\pi}{\beta_1 \sin\theta_{\text{in}}}. \tag{35}$$

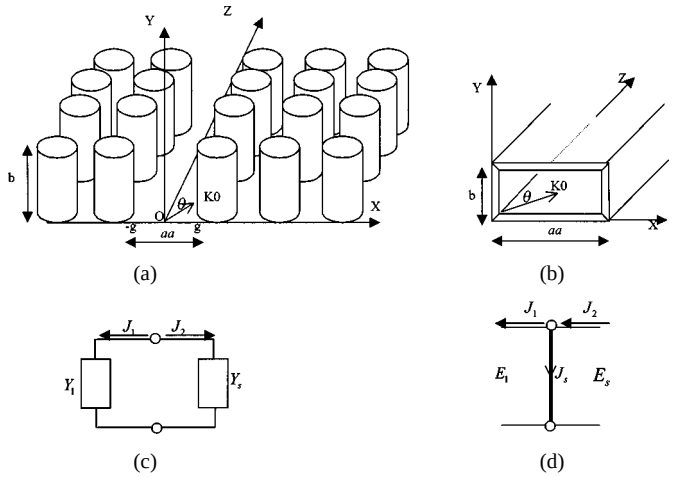

Fig. 7. (a) Geometry of waveguide between two grids of metallic holes ($aa = 20$ mm). (b) Rectangular waveguide length a and height b. (c) Equivalent circuit of the waveguide with Y_s is the surface admittance and Y_1 is the admittance of the magnetic wall in $x = 0$. (d) Diagram of continuity conditions.

Thus, one can place the second metal surface (perfect electric conductor) in one of these planes without disturbing the fields. The distance aa between these two planes is fixed so one can deduce the angle of incidence as

$$\theta_{\text{in}} = \arcsin\left(\frac{m \cdot \pi}{\beta_1 \cdot aa}\right). \tag{36}$$

In order to define this angle, it is necessary that the term between brackets be less than one, and one must have

$$aa \geq \frac{m\pi}{\beta_1} = \frac{m\pi}{\omega\sqrt{\varepsilon_0\mu_0}} = \frac{m\lambda_0}{2}. \tag{37}$$

The distance between two metallic surfaces must be larger than the half-wavelength so that the conditions are satisfied. As the electric field is directed along to y, one can place a metallic plane perpendicular to this direction without disturbing the electromagnetic field, in a plane of constant y. If one places two planes at $y = 0$ and $y = b$, in addition to the two planes already placed at $x = 0$ and $x = aa$, one forms a rectangular metallic waveguide [see Fig. 7(b)]. The addition of three metallic planes does not modify the structure of the fields inside the waveguide, which are given by the reflection and transmission of the factors [22].

The propagation in the guide is in the z-direction and one notes that, if the electric field is perpendicular to this direction, the magnetic field has, on the other hand, a longitudinal component. With this condition, one can say that the mode is TE. The propagation constant along the guide is defined by the x dependence of the fields

$$\begin{aligned}\beta =& \frac{2 \cdot \pi}{\lambda_g} = \beta_1 \cos\theta_{\text{in}} = \beta_1\sqrt{1 - \sin^2\theta_{\text{in}}} \\ =& \beta_1 \cdot \sqrt{1 - \left(\frac{m\pi}{\beta_1 aa}\right)^2}\end{aligned} \tag{38}$$

where λ_g is the guided wavelength.

Recently, 2-D periodic structures have attracted considerable attention in the literature, though often under the new name of "photonic-bandgap (PBG) structures [23]. Experimental data are compared with scattering parameter calculated data on the basis of suitable form of the 2-D Helmholtz equation for metallic propagation media [24]. Experimental and theoretical study of frequency-selective coupling properties of waveguide-based structures patterned in a metallic photonic crystal is given in [25]. A rigorous analysis is presented for the guiding of wave by a 2-D periodic impedance surfaces [26]. The approximation of a periodic structure by an impedance surface had been successfully employed for the study of 1-D periodic structures [27], and this work can be considered as an extension of the earlier work to the 2-D case.

In this paper, a novel technique in microwave circuit design is to build an isolation screen using metallic holes, which are periodically arranged in a 2-D grid. Using this approach, the waveguide is established between two grids of periodically arranged metallic plates, as shown in Fig. 7(a), where these metallic plates act as a continuous wall. The waveguide is limited between $x = -g$ and $x = g$and, thus, it can be considered a homogeneous waveguide, which has a straight section YOZ, and short circuit at $x = g$, and the same consideration for the negative direction $-x$. Let us suppose the electric field at level oz is equal to E for $x > 0$. The magnetic field J_1 on the right-hand side can be deduced in the same way as J_2 on the left-hand side $x < 0$ can be deduced. The equation of the continuity for the H-field is applied on J and, therefore, it permits the determination of the dispersion equation. For the waveguide that has a short circuit at the distance g and directed to the load, one can write $\vec{J} = \vec{H} \wedge \vec{n}$ and $\vec{J} = Y\vec{E}$.

To examine the continuity conditions at the crossing of the surface, let us take the general case, which is a current surface

$$E_{1t} = E_{2t} \tag{39}$$

$$\vec{H}_{1t} - \vec{H}_{2t} = \vec{J}_s \wedge \vec{n} \text{ with } \vec{J}_1 - \vec{J}_2 = -\vec{J}_s. \tag{40}$$

The continuity conditions are verified in Fig. 7(c). The arch covered by J_s is not a short circuit, but, in the general case, an impedance. Let us take again the problem of Fig. 7(a). The method presented above allows the equivalent circuit shown in Fig. 7(b). The orientations of J_1 and J_2 are now different. The continuity of H is expressed, therefore, by o, k.

$$\vec{J}_1 + \vec{J}_2 = 0 \tag{41}$$

$$Y_1 + Y_s = 0 \tag{42}$$

where $Y_1 = Y_m \cdot \text{th}(\gamma_n \cdot g)$ is the admittance of an open circuit at a magnetic wall in $x = 0$, and Y_s is the surface admittance of the periodically arranged metallic holes.

The propagation in the guide is in the z-direction, and one notes that if the electric field is perpendicular to this direction, the magnetic field has a longitudinal component. Consider the transverse resonance for the TE mode. Substituting the admittance of electric mode TE in (42), one obtains

$$\frac{\gamma_n}{j\omega\mu}\text{th}(\gamma_n\, g) + Y_s = 0. \tag{43}$$

Put $Y_s = j \cdot X_s$ (X_s is the imaginary part of the admittance surface, which depends on the incidence angle), where the associated transverse propagation constant in the metallic holes arranged periodically is given by

$$\beta_{nx} = k_0 \sin\theta + \frac{2n\pi}{a} \text{ and } Y_1 = \frac{j\beta_n}{\omega\mu} tg(\beta_n g).$$

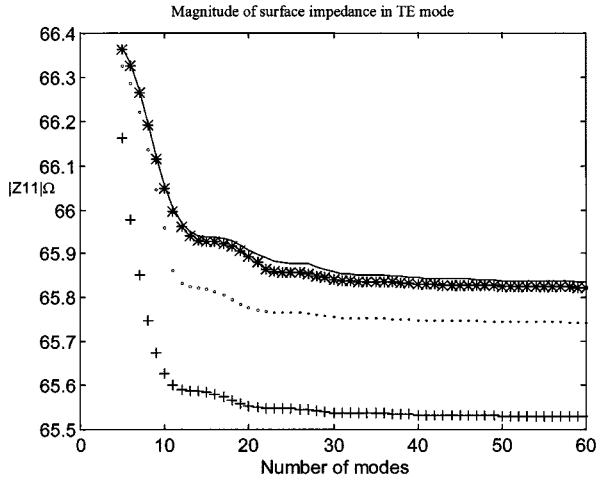

Fig. 8. Magnitude of surface impedance Z_{11} for eight metallic holes cascaded in a periodic guide as a function of the number of modes with $\theta \approx 0$, $f = 10$ GHz, and trial functions $(p) = (++10, \cdots 20, —40, ** 50)$.

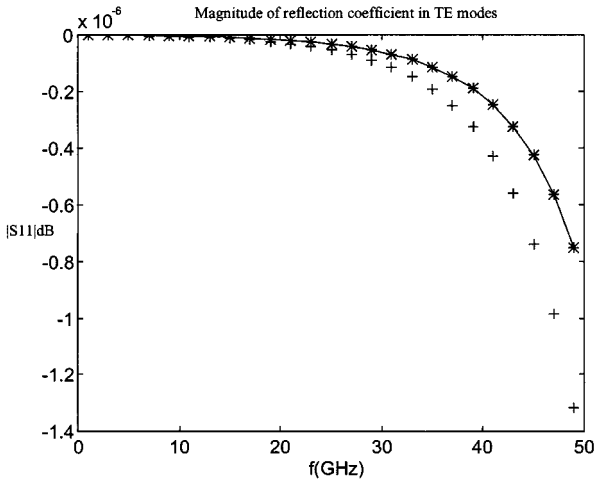

Fig. 9. Magnitude of reflection coefficient S_{11} for eight metallic holes cascaded in a periodic guide as a function of the frequency with $\theta \approx 0, p = 40$, and $n = 40$ for $(++3, —5, ** 11)$ accessible modes.

Therefore, the equation of dispersion becomes

$$\beta_n tg(\beta_n g) + \omega\mu X_s = 0 \tag{44}$$

where $\beta_n = k_0 \sin\theta_{\text{in}}$, $\sin\theta_{\text{in}} = \beta_n/k_0$, and the propagation constant in the z-direction for a waveguide that is presented in Fig. 7(a) can be defined as

$$\beta_z = k_0 \cos\theta_{\text{in}} = k_0\sqrt{1 - \left(\frac{\beta_n}{k_0}\right)^2}. \tag{45}$$

Considering the boundary conditions, the TE field can be written as

$$E_y = E_0 \cos(\beta_n x) e^{-j\beta_z z}. \tag{46}$$

VIII. Numerical Results and Discussions

To test the convergence behavior of the technique, the magnitude of the surface impedance $|Z_{11}|$ as a function of the number of modes and trial functions has been studied for square and truncated square slabs in order to optimize a number of them. Fig. 8 illustrates the convergence magnitude of the surface impedance $|Z_{11}|$ for the structure shown in Fig. 1 in case of a TE mode for eight square plates in cascade as a function of number of modes. It can be noticed that 40 trial functions (p) and 40 modes (n) are sufficient to give good convergence. This model is applicable by using five accessible modes since the results of five accessible modes give the same results as more than five, as shown in Fig. 9. The dimension parameters of the structure are $a = 1$ mm, the incident angle is $\theta \approx 0$, and the length of the square metallic slabs is $b = 0.1$ mm.

The convergence magnitude of the surface impedance $|Z_{11}|$ for the truncated square slabs for eight plates in cascade in the TE mode as a function of number of modes is also treated in the same manner. The convergence becomes good for 40 modes and 40 trial functions at the level of the first discontinuity p_1 and ten trial functions at the level of the second discontinuity p_2 for five accessible modes. On the other hand, for the truncated square slabs, the dimension parameters of this structure are $a = 1$ mm, incident angle $\theta \approx 0$, and the dimensions of one metallic slabs

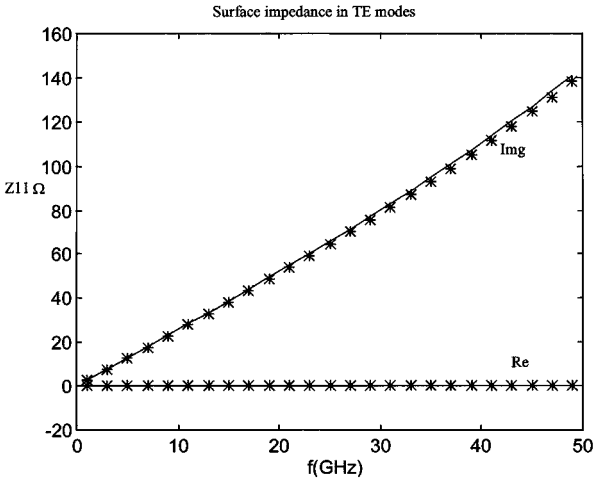

Fig. 10. Imaginary and real parts of the surface impedance for eight metallic holes cascaded in a periodic guide for the geometry of square and truncated square approaches versus frequency with $\theta \approx 0, p = 40, p_2 = 10, p_1 = 40$, and $n = 40$ (square approach — and truncated square approach $***$).

are $d = 0.017$ mm, and $b = 0.072$ mm. The same dimensions, trial functions, accessible modes, and number of modes will be used in Section IX.

A comparison between the imaginary and real part of the surface impedance $|Z_{11}|$ of square and truncated square slabs in a periodic guide for the same surface are presented in the following figures. The presentation of the imaginary and real part of the surface impedance for the eight ranges of the metallic holes in cascaded Fig. 1, which are approximated by the square and truncated square slabs, is presented in Fig. 10 for TE modes. The results obtained for the imaginary part of the surface impedance of the eight slabs have approximately the same values for the two approaches and they increase when the frequency is increased and the real part of the surface impedance are equal to zero for the two approaches. The eight ranges in cascade in a periodic guide are sufficient to obtain good isolation. The magnitude of the reflection coefficient $|S_{11}|$ and $|S_{12}|$ for TE modes versus the operating frequency are plotted in Fig. 11 for eight metallic slabs in cascade in

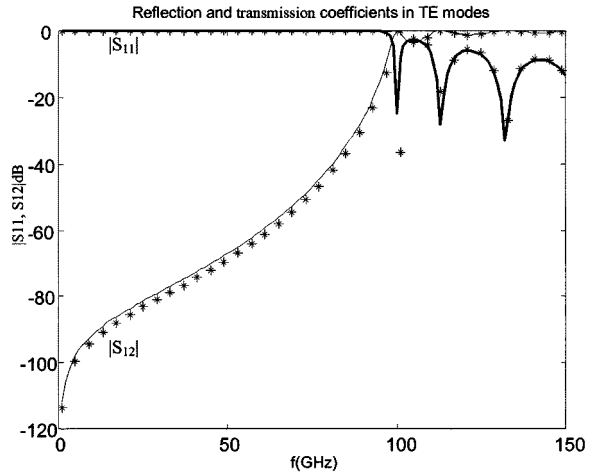

Fig. 11. Magnitude of reflection and transmission coefficients for eight metallic holes cascaded in a periodic guide for the geometry of square and truncated square approaches versus frequency with $\theta \approx 0, p = 40, p_2 = 10$, $p_1 = 40$, and $n = 40$ (square approach —, and truncated square approach $***$).

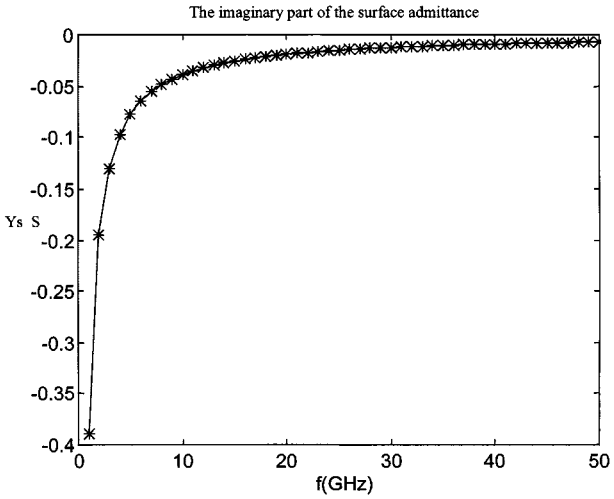

Fig. 12. Imaginary part of surface admittance for eight metallic holes disposed in cascade in a periodic guide versus the frequency for an incident angle ($\theta \approx 0$ — and $\theta \approx 90 * **$).

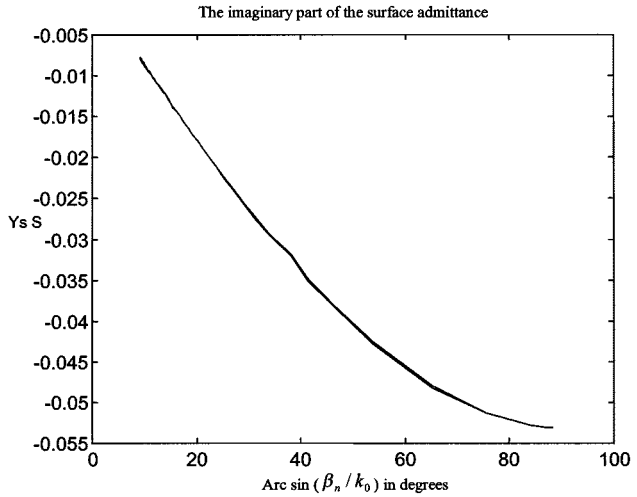

Fig. 13. Variation of the imaginary part of the surface admittance for eight metallic holes disposed in cascade in a periodic guide with the incident angle θ_{in}, which present the relation of the constant of propagation β_n with k_0 inside the waveguide design between two grids of periodically arranged metallic holes, as in Fig. 7(a).

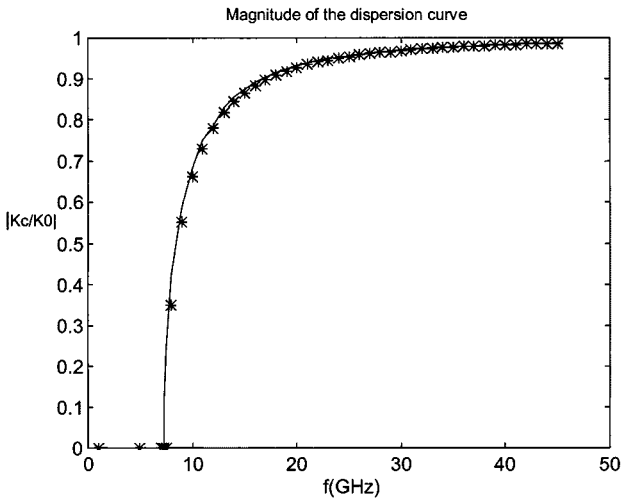

Fig. 14. Magnitude of dispersion curve for geometry of Fig. 7(b) $***$ and Fig. 7(a) — versus frequency.

a periodic guide. The comparison shows that the magnitude of the reflection coefficient increased when the frequency increased and, on the other hand, the transmission coefficient increased with frequency. From this result, the isolation is satisfied for replacing the continuous structure by the metallic holes arranged periodically (Fig. 1) for frequencies less than 50 GHz. For this domain, the imaginary part of the surface admittance is plotted for the incident angles of 0° and 90°, as in Fig. 12. The results obtained for the imaginary part of the surface admittance of the eight slabs are approximately the same values for the two incident angles. Also, the comparison between the reflection coefficient for the two incident angles gives less than 1 dB in that domain. The calculation of the dispersion curve in the waveguide, which is built from the metallic holes arranged periodically, is presented in (44). This equation give the surface admittance that is dependent on the constant of propagation in the x-direction (β_n) and the free-space number (k_0); for this reason, Fig. 13 illustrates the imaginary part of surface admittance Y_s as a function of $\arcsin(\beta_n/k_0)$. In this figure, the amplitude of the imaginary part of the surface admittance increased with (β_n/k_0). From (45), the magnitudes of the dispersion curve for Fig. 7(a) versus the operating frequency is plotted in Fig. 14. The dispersion curves represent the propagation constants, and the cutoff frequencies of the waveguide for the fundamental mode. Also in this figure, the dispersion curves represent the propagation constant for a rectangular waveguide [see Fig. 7(b)], which has the same proportion (dimensions that verify the condition (37) for the incidence angle). The comparisons between the two curves give approximately the same values, which allows one to build a waveguide from the metallic holes arranged periodically. Fig. 15 shows the magnitude of transmission coefficient obtained in the theoretical and experimental case for the first propagating mode in the waveguide, which is made up between two grids of periodically arranged metallic plates [see Fig. 7(a)]. By considering an equivalent waveguide of width $aa = 2$ cm, the dimension parameters of the theoretical study are $a = 5$ mm and

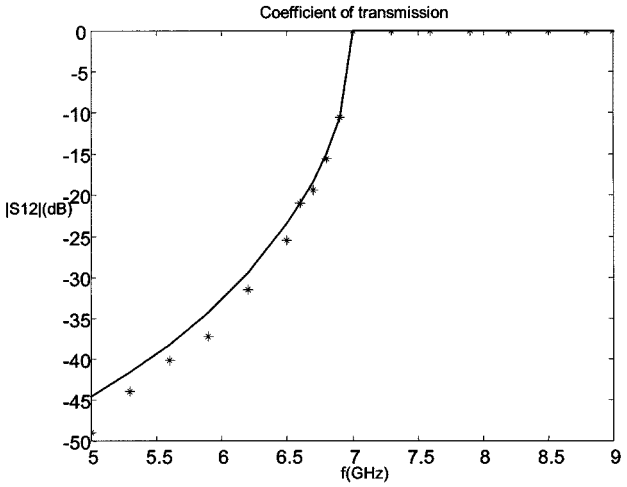

Fig. 15. Magnitude of transmission coefficient for geometry of Fig. 7(a) versus frequency (theoretical — and experimental $***$).

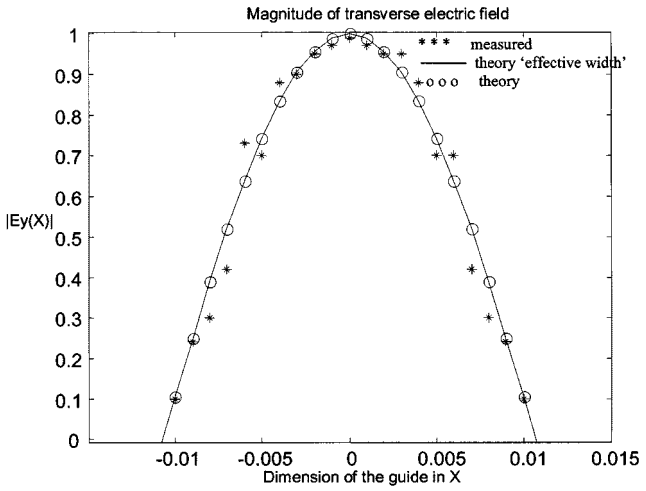

Fig. 16. Variation of the TE field for geometry of Fig. 7(a) for the fundamental mode (theoretical ooo, experimental $***$, and theoretical effective width —).

$b = 1.22$ mm, and the experimental study are $a = 5$ mm and the diameter of wires $D = 1.38$ mm. The cutoff frequency in both cases is conforming, but this frequency does not correspond to a classic waveguide, which has the same width. Fig. 16 depicts the magnitude of the TE field E_y theoretically and experimentally for the dominant TE_{10} mode inside the waveguide, which is built from the metallic holes, arranged periodically. The dimension parameters are as noted above. The electric field does not begin from zero on the metallic holes because of the values of the surface admittance. For this reason, Fig. 16 shows the magnitude of the electric field, which gives the effective width; this width corresponds to the cutoff frequency in Fig. 15.

A comparison between the reduced transfer impedance magnitude $|Z_{12}|$ of circle, square, and truncated square cross sections in a rectangular guide for the same surface are presented in Fig. 17. A study was realized in order to justify the proposed suggestion. The dimension parameters of the structure are $a = 2.2$ cm, the length of the square metallic plates is $b = 1.77$ mm, and for the truncated square metallic plates is $b = 1.27$ mm and $d = 0.3$ mm (the diameter of the circle that

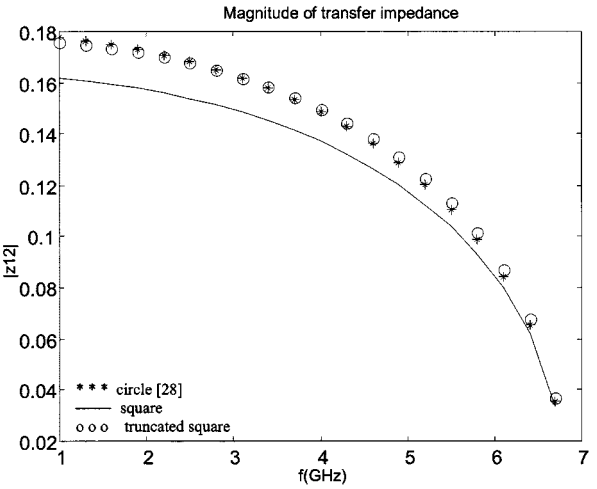

Fig. 17. Magnitude of reduced Z_{12} for a circle, square, and truncated square metallic obstacle in a rectangular guide versus frequency with: circle diameter $D = 2$ mm, $b = 1.77$ mm for square, and $b = 1.27$ mm and $d = 0.3$ mm for a truncated square for TE modes.

has the same surface is $D = 2$ mm). For this structure, it can be noticed that ten trial functions for all discontinuity, and 25 modes are sufficient to give good convergence. The dependence of the magnitude of the transfer impedance versus frequency for the TE mode of the three structures is shown in Fig. 17. From this figure, one can notice that the three curves have the same shape and approximately the same values for circular and truncated square forms. A very good agreement with the literature results given in [28] is demonstrated. In a periodic waveguide, the accuracy of the analysis is demonstrated by a comparison between theoretical results and experimental ones for via-holes with a circular cross section of the same surface [29].

IX. Conclusions

The problem of arbitrarily incident plane-wave scattering from strip structures of thick conducting plates arranged with 2-D periodicity has been examined in this paper. The square approximation, as well as truncated square approximation of circular cross sections has been used in this study. The impedance of cascaded screens and the reflection coefficient was calculated using the multimodal variational method for both the TE- and TM-polarized incident electric fields. The 2-D periodic strip of holes described in this paper can be used for the purpose of designing new microwave guiding structures. A transverse resonance method has been applied in order to solve this problem. A fast rate of convergence with an increasing number of modes and trial functions has been demonstrated for TE modes of the two cases. The numerical results of the two cases have been compared with each other. The conclusion drawn from this investigation is that the two uses of the waveguide mode of square metallic plates screen or truncated square metallic plates exhibit the same performance concerning their reflection coefficient. The best surface impedance was obtained in the case of a cascaded discontinuities configuration of the waveguide. The given close analysis of periodically arranged metallic holes showed that this arrangement can be used for the design of new microwave waveguide structures.

REFERENCES

[1] R. E. Collin, *Field Theory of Guide Waves*. New York: McGraw-Hill.

[2] R. H. Ott, R. G. Kouyoumjian, and L. Peters, Jr., "Scattering by a two-dimensional periodic array of narrow plates," *Radio Sci.*, vol. 2, pp. 1347–1349, Nov. 1967.

[3] R. B. Kieburtz and A. Ishimaru, "Scattering by a periodically apertured conducting screen," *IRE Trans. Antennas Propagat.*, vol. AP-9, pp. 506–514, Nov. 1961.

[4] T. Cwik and R. Mittra, "The cascade connection of planar periodic surface and lossy dielectric layers to form and arbitrary periodic screen," *IEEE Trans. Antennas Propagat.*, vol. AP-35, pp. 1397–1405, Dec. 1987.

[5] B. J. Rubin and H. L. Bertoni, "Scattering from a periodic array of conducting bars of finite surface resistance," *Radio Sci.*, vol. 20, no. 4, pp. 827–832, July–Aug. 1985.

[6] B. J. Rubin, "Scattering from a periodic array of apertures or plates where the conductors have arbitrary shape, thickness and resistivity," *IEEE Trans. Antennas Propagat.*, vol. AP-34, pp. 1356–1365, Nov. 1986.

[7] N. Amitay and V. Galindo, "The analysis of circular waveguide phase arrays," *Bell Syst. Tech. J.*, vol. 47, pp. 1903–1932, Nov. 1968.

[8] R. F. Harrington, *Time–Harmonic Electromagnetic Fields*. New York: McGraw-Hill, 1961, pp. 129–132.

[9] T. E. Rozzi and W. F. G. Mecklenbruker, "Wide-band net work modeling of interacting inductive irises and step," *IEEE Trans. Microwave Theory Tech.*, vol. MTT-23, pp. 235–245, Feb. 1975.

[10] T. E. Rozzi, "Network analysis of strongly coupled transverse apertures in waveguide," *Int. J. Circuit Theory Applicat.*, vol. 1, pp. 161–179, 1972.

[11] F. Bouzidi, H. Aubert, D. Bajon, and H. Baudrand, "Equivalent network representation of boundary conditions involving generalized trial quantities—Application to lossy finite metallization thickness," *IEEE Trans. Microwave Theory Tech.*, vol. 45, pp. 869–876, June 1997.

[12] H. Baudrand, H. Aubert, D. Bajon, and F. Bouzidi, "Equivalent network representation of boundary conditions involving generalized trial quantities," *Ann. Telecommun.*, vol. 52, no. 5–6, pp. 285–292, 1997.

[13] H. Baudrand and H. Aubert, "Integral formulation for planar active or passive devices using equivalent circuit approach," presented at the IEEE MTT-S Int. Microwave Symp. Workshop, San Francisco, CA, 1996.

[14] H. Aubert and H. Baudrand, "Origin and avoidance of spurious solutions in transverse resonance method," *IEEE Trans. Microwave Theory Tech.*, vol. 41, pp. 450–456, Mar. 1993.

[15] H. Baudrand, "Representation by equivalent circuit of the integral methods in microwave passive elements," in *20th Eur. Microwave Conf.*, Budapest, Hungary, Sept. 1990, pp. 1359–1364.

[16] M. Nadarassin, H. Aubert, and H. Baudrand, "Analysis of planar structures by an integral approach using entire domain trial functions," *IEEE Trans. Microwave Theory Tech.*, vol. 10, pp. 2492–2495, Oct. 1995.

[17] ——, "Analysis of planar structures by an integral multi-scale approach," in *IEEE MTT-S Int. Microwave Symp. Dig.*, vol. 2, Orlando, FL, May 14–19, 1995, pp. 653–656.

[18] J. W. Tao and H. Baudrand, "Multimodal variational analysis of uniaxial wave guide discontinuities," *IEEE Trans. Microwave Theory Tech.*, vol. 39, pp. 506–516, Mar. 1991.

[19] P. Couffignal, H. Baudrand, and B. Thern, "A new rigorous method for the determination of iris dimensions in dual-mode cavity filters," *IEEE Trans. Microwave Theory Tech.*, vol. 42, pp. 1314–1320, July. 1994.

[20] R. Mittra and S. W. Lee, *Analytical Techniques in the Theory of Guided Waves*. New York: Macmillan, 1971.

[21] R. Sorrentino, "Planar circuits, waveguide models, and segmentation method," *IEEE Trans. Microwave Theory Tech.*, vol. MTT-33, pp. 1057–1066, Oct. 1985.

[22] F. Gardiol, *Traite d'Electricite—Electromagnetism*. Lausanne, France: Presse Polytech. Romandes, 1996, vol. III, pp. 160–170.

[23] V. Radisic, Y. Qian, R. Coccioli, and T. Itoh, "Novel 2-D photonic bandgap structures for microstrip lines," *IEEE Microwave Guided Wave Lett.*, vol. 6, pp. 69–71, Feb. 1998.

[24] J. Danglot, J. Carbonell, M. Fernandez, O. Vanbesien, and D. Lippens, "Modal analysis of guiding structures patterned in metallic photonic crystal," *Appl. Phys. Lett.*, vol. 73, pp. 2712–2714, Nov. 1998.

[25] J. Danglot, O. Vanbesien, and D. Lippens, "A 4-port resonant switch patterned in photonic crystal," *IEEE Microwave Guided Wave Lett.*, vol. 9, pp. 274–276, Nov. 1999.

[26] S. T. Peng and R. B. Hwang, "Analysis of two-dimensionally periodic structures graphical methods and physical consequences," in *29th Eur. Microwave Conf.*, Munich, Germany, Oct. 1999, pp. 299–302.

[27] Hessel and A. A. Oliner, "A new theory of Wood's anomalies on optical gratings," *Appl. Opt.*, vol. 4, pp. 1275–1297, 1965.

[28] N. Marcuvitz, *Waveguide Handbook*. Stevenage, U.K.: Peregrinus, 1986, pp. 257–263.

[29] A. Zeid and H. Baudrand, "Electromagnetic shielding using several cascaded metallic holes for applications in microwave circuits," in *30th Eur. Microwave Conf.*, Paris, France, Oct. 2000, pp. 138–141.

Ali Zeid (S'00–A'00) was born in Salamia, Syria, in 1965. He received the Dipl.-Ing. degree from the University of Teshreen, Teshreen, Syria, in 1995, and the DEA and Ph.D. degrees from the National Polytechnic Institute, Toulouse, France, in 1996 and 2001, respectively.

He is currently a Professor in the Department of Telecommunication, Faculty of Electric and Electronic Engineering, University of Allepo, Allepo, Syria. His research interest is in numerical modeling of microwave and millimeter-wave structures, particularly applications to telecommunication systems.

Henri Baudrand (M'86–SM'90) was born in Chatou, France, in 1939. He received the Dipl.Ing. and Ph.D. degrees from the National Polytechnic Institute, Toulouse, France, in 1962 and 1966, respectively.

Since 1966, he has been involved with the modeling of active and passive microwave circuits by integral methods in the Electronic Laboratory, ENSEEHIT, Toulouse, France, where he is currently a Professor of microwaves in charge of the Microwave Research Group. He has authored or co-authored over 100 papers in journals, 250 papers in international meetings, *Introduction au calcul des éléments de circuits passifs en hyperfréquences* [tomes I and II (exercises)], and *Conception de circuits linéaires et non linéaires en microondes* (editions CEPADUES).

Dr. Baudrand is a Doctor Honoris Cause of University Iasi. He was chairman of the French chapter of the IEEE Microwave Theory and Techniques Society (IEEE MTT-S) and the IEEE Electron Devices Society from 1996 to 1998.